



HAL
open science

Nematic polymers: hairpins, ringlets and excimer fluorescence

D. Williams, A. Halperin

► **To cite this version:**

D. Williams, A. Halperin. Nematic polymers: hairpins, ringlets and excimer fluorescence. Journal de Physique II, 1993, 3 (1), pp.69-89. 10.1051/jp2:1993112 . jpa-00247814

HAL Id: jpa-00247814

<https://hal.science/jpa-00247814>

Submitted on 4 Feb 2008

HAL is a multi-disciplinary open access archive for the deposit and dissemination of scientific research documents, whether they are published or not. The documents may come from teaching and research institutions in France or abroad, or from public or private research centers.

L'archive ouverte pluridisciplinaire **HAL**, est destinée au dépôt et à la diffusion de documents scientifiques de niveau recherche, publiés ou non, émanant des établissements d'enseignement et de recherche français ou étrangers, des laboratoires publics ou privés.

Classification

Physics Abstracts

36.20c — 61.30B — 82.35

Nematic polymers: hairpins, ringlets and excimer fluorescence

D.R.M. Williams and A. Halperin

Department of Materials, University of California, Santa Barbara, CA 93106, U.S.A.

(Received 3 July 1992, revised 12 October 1992, accepted 19 October 1992)

Abstract. — Short liquid crystalline polymers in a nematic environment are very unlikely to cyclise. Hairpins, abrupt chain folds, favour cyclisation. As a result the cyclisation rate constant exhibits a maximum as a function of chain length. The maximum corresponds to a new object, a “ringlet”. The rate constant also depends exponentially on temperature. This suggests excimer fluorescence as a probe of configurations and dynamics of main-chain liquid crystalline polymers.

1. Introduction.

Main chain nematic polymer liquid crystals (PLCs) are long molecules with nematic mesogens in the backbone. They are of commercial importance because of their role in the production of strong fibres. Their scientific interest is due to the combination of the intrinsic random nature of polymers with the ordering inherent in liquid crystals [1, 2]. Here we will be mainly concerned with wormlike PLCs in which the mesogens are separated by flexible spacers. These obey Gaussian statistics in the isotropic melt regime but are deformed in the nematic phase. They can exhibit “hairpins” which are rapid reversals in the direction of the chain (Fig. 1). The hairpins are joined by chain segments which, on average are well aligned with the nematic field. Hairpins represent a thermally excited state of the chain, whose ground state is that of a rod perfectly aligned with the nematic director. In forming hairpins the chain pays an energy penalty due to chain elasticity and the nematic field, but gains configurational entropy. Previous theoretical work has suggested hairpins might manifest themselves in dielectric response, NMR and elasticity [3-6], yet there is no *clear* experimental evidence for their existence. In the following we consider the effect of *hairpins* on *cyclisation* with special emphasis on excimer formation in chains end-capped by two fluorescent tags. The analysis suggests that the integrated intensity of the excimer emission \mathcal{I} , provides a clear test for the existence of hairpins. In particular: (1) \mathcal{I} exhibits a sharp maximum as a function of N , the degree of polymerisation. As we shall see this maximum is due to a new object - a “ringlet”. (2) \mathcal{I} increases with temperature with an exponential type dependence. In marked distinction \mathcal{I} for a flexible chain [7-15] in an isotropic melt is expected to decrease monotonically with N while exhibiting

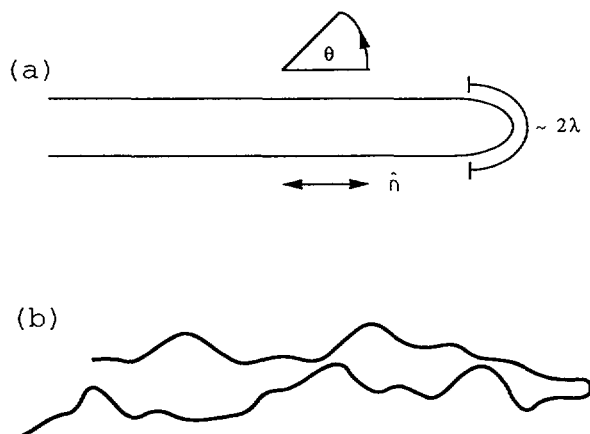


Fig.1. — (a) A sketch of an ideal hairpin. The nematic director is represented by \hat{n} , and the length of the bend is of the order of a hairpin length λ . In reality, because of thermal fluctuations the arms meander perpendicular to the nematic director and produce a hairpin looking more like (b). In general the perpendicular extent is due to small chain meanders and is not caused by the lateral extent of the hairpin bend. Despite this the arms are in fact straight to a good approximation.

weak temperature dependence. The cyclisation of PLCs is thus of interest both because of its distinctive features *vis-a-vis* the isotropic melt case and as a probe of chain configurations.

The primary aim of this paper is to study the effect of hairpins on cyclisation experiments. In such an experiment one joins the two ends of some labelled polymer chains [16], either temporarily or permanently. For the two ends to join they must approach within a small distance - the capture radius. The starting point of this paper is one simple fact. In a chain with a hairpin the two ends of a *single* chain can be very close together, whereas in rod this is not possible. Rods can only react *via* intermolecular contact, whereas hairpinned chains can cyclise. This means that if the concentration of labelled chains is small the amount of cyclisation will be greatly increased by the presence of hairpins. Exciplex or excimer fluorescence [17] provide an efficient probe for this effect. The basic idea is demonstrated in figure 2. One first labels some chains by attaching fluorescent groups A and B to their ends. Pyrene groups have been previously used for this purpose. These are then placed in an unlabelled melt or solution, which is illuminated by a short pulse of light of appropriate wavelength. This light excites say A to some new state A^* . This excited state can then follow two possible paths. Either the ends spontaneously relax to their ground state, emitting radiation with a broad spectrum. This occurs with characteristic time τ_s . Alternatively, the A^* and B ends meet and cyclise the chain, forming an $(AB)^*$ complex. This then emits radiation with a spectrum different from the spontaneous emission, and one returns to an open chain state. This is called exciplex emission if the A and B are different, and excimer emission if A and B are the same. The characteristic time for decay by this mode we call τ_E . The reverse reaction $(AB)^* \rightarrow A + B$ is assumed to be highly improbable and we do not consider its effects here. The idea is to measure the excimer or exciplex output from the reaction $(AB)^* \rightarrow A + B$. By integrating the signal from the excimer radiation with respect to time one gets an idea of how many ends have met. Ideally one would like τ_s to be fairly large. This would give many chain ends enough time to meet one another and promptly emit some excimer radiation [13].

Fluorescence has been used in many experimental studies of diffusion controlled reaction for

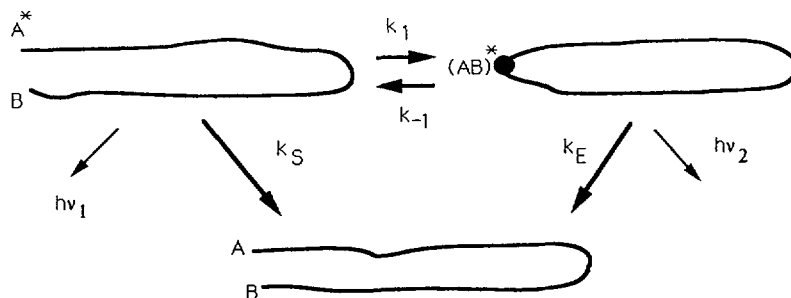


Fig.2. — The general excimer reaction diagram. An excited A^* end can either decay spontaneously with rate constant k_s emitting radiation of frequency ν_1 (usually in a broad spectrum). Alternatively, if it meets a B end the chain can cyclise and then emit excimer radiation and decay again to the ground state, with rate constant k_E .

polymers [16-19]. The kinetics are as follows. The time t is measured from the initial light pulse used to excite the A to A^* . We designate the density of unreacted A^* ends at any time as $[A^*]$. This density decays in time because of two processes. Firstly, excimer formation can take place via the reaction $A^* + B \rightarrow (AB)^*$. Secondly, spontaneous decay can take place, $A^* \rightarrow A$. These two processes have associated reaction constants $k(t)$ and $k_s = 1/\tau_s$, so that $[A^*]$ satisfies

$$\frac{d[A^*]}{dt} = -(k(t) + k_s)[A^*]. \quad (1)$$

We are concerned here only with those ends which form excimers, i.e. in the contribution characterised by $k(t)$. We thus define a new density of ends $n(t)$ so that dn/dt is the rate at which labelled ends are meeting, even though some of them have already decayed spontaneously. The instantaneous signal is caused only by those ends which have not decayed, and is thus proportional to $\exp(-t/\tau_s) \frac{dn}{dt}$. It turns out that the simplest quantity of interest is the integrated intensity \mathcal{I} which is the Laplace transform of $\frac{dn}{dt}$

$$\mathcal{I} \propto \int_0^\infty dt \exp(-t/\tau_s) \frac{dn}{dt} \quad (2)$$

By concentrating on \mathcal{I} we have ignored most of the time-dependent information in the problem. We can of course include this later by examining the instantaneous signal. We will be mainly interested in the dependence of \mathcal{I} on N and the temperature T . Because of the exponential spontaneous decay of the excited ends only those ends that create excimers in a time of order a few τ_s contribute significantly to the measured \mathcal{I} . The integrated intensity \mathcal{I} also avoids any complications arising from the finite lifetime τ_E of the excimers.

We begin our discussion with a brief review of the statics and dynamics of hairpins. Their long term "reptative" dynamics are discussed in section 3. The effect of hairpins on cyclisation and fluorescence is considered in section 4. In section 5 a new kind of entity, a "ringlet", is introduced. This is a short cyclised chain with length of a few hairpin lengths. It is formed by the chain whose length has the maximum cyclisation rate at fixed temperature.

2. A brief review of hairpins.

Nematic PLCs are often conceptualised as wormlike chains. A truly wormlike chain can bend, but cannot stretch. Usually such chains are modelled in a smeared out continuum fashion so that a length of chain s possesses both nematic and flexible properties. The energy functional for a given chain then consists of two terms. Firstly there is a nematic term which favours the alignment of the chain with the director $\pm \hat{n}$. This effect is usually modelled as a mean field which is caused by the surrounding molecules. Secondly there is a bending term allowing for the energy penalty the polymer pays for bending. The lowest energy trajectory for any chain is then a straight line aligned along the director. However, at finite temperature there will always be deviations from this in the form of small wiggles. These are one way in which the chain can store both energy and entropy. There is a second, more interesting way, first suggested by de Gennes [20], and this is for the chain to undergo rapid reversals in direction called "hairpins" [20, 3, 21, 4, 22, 6, 23-31]. An example is shown in figure 1. The hairpin trajectory is obtained by extremising the energy functional, and is a mechanical equilibrium state of the chain. The hairpin bend represents a balance between the bending term, which favours slow bending and the nematic term, which promotes rapid folding so that the chain runs perpendicular to the field for only a short distance.

The energy functional of a chain of length L in a plane with $\theta(s)$ specifying the angle a monomer of arc position s makes with the director is

$$U[\theta(s)] = \frac{1}{2} \int_0^L ds \left[\epsilon \left(\frac{d\theta}{ds} \right)^2 + 3aS \sin^2 \theta(s) \right], \quad (3)$$

where a is the nematic coupling constant, S the order parameter, and ϵ the bending constant. The hairpin shape is specified by the Euler-Lagrange equation corresponding to (3). This yields a pendulum-type equation whose solution for an infinitely long chain is

$$\theta(s) = 2 \tan^{-1}[\exp(s/\lambda)] \quad s \in (-\infty, \infty). \quad (4)$$

This represents a soliton-like disturbance (Fig. 1). The characteristic length associated with a hairpin (i.e. roughly the length of the bend), and its energy are respectively

$$\lambda = \left(\frac{\epsilon}{3aS} \right)^{1/2} \quad U_h = 2(3aS\epsilon)^{1/2} \quad (5)$$

Almost all the energy is localised around the bend, and from (20) the angle made by the chain with the director exponentially approaches zero $\sim \exp(-s/\lambda)$ where s is the distance from the bend. Although hairpins are mechanical equilibrium states they are in fact weakly unstable. The unstable mode consists of shuffling length from one arm to the other until the hairpin bend is near the end of the chain, where it rapidly falls off. The potential driving this instability is very weak and the motion can be considered as free diffusion unless the temperature is very low. One should note that although hairpins are unstable one still expects them to exist by thermal excitation. It is possible to put more than one hairpin on a chain of length L , up to a maximum number $\sim L/(\pi\lambda)$. If two hairpins on a single chain are separated by more than a few λ they will attract each other exponentially weakly. Close encounters can result in mutual annihilation. Hairpins have a major geometrical effect on a chain. For a chain with n hairpins the end-to-end displacement measured along the director varies like $\sim Ln^{-1/2}$.

A simple model for the hairpin distribution function is to treat the hairpin bends as a one-dimensional, non-interacting ideal gas as first proposed by de Gennes [20], and refined by Gunn

and Warner [3, 21]. The partition function for a chain with n hairpins is $z(n) = \Gamma^n/n!$ with Γ

$$\Gamma = \frac{L}{l} \exp(-U_h/k_B T) \quad (6)$$

Here l is a length arising for the intrinsic degree of wobbling of the chain and sets the limit to which one can define the position of a hairpin [21]. To calculate it one must go beyond the confines of the ideal gas model, the result is [21]

$$l = \frac{k_B T}{24aS} \quad (7)$$

We note that l is roughly the ratio of $k_B T$ to the energy in the first wigggle eignemode of the chain [4]. The length L is analogous to the volume in an ordinary gas. One should note that this gas is rather like a photon gas - the number of hairpins is not conserved. The probability of finding n hairpins on a chain of length L is then

$$P(n) = \exp(-\Gamma) \frac{\Gamma^n}{n!} \quad (8)$$

and the average number of hairpins on a chain is $\langle n \rangle = \Gamma$, the standard deviation being $\sqrt{\Gamma}$. The distribution for $\Gamma > 1$ is peaked about $n \approx \Gamma$ i.e about the average. One should note that for an average population of one hairpin per chain the probability distribution is just $P(n) = e^{-1}/n!$ so that $P(0) = P(1)$ and there are just as many zero-hairpin chains as one-hairpin chains, while the number of chains with large numbers of hairpins decays very rapidly. The ideal gas analogy applies only in the case where the degree of wobbling is small and hairpins are well defined.

So far we have pictured hairpins as two rods joined by a short bend. In reality the rods are not perfectly straight and parallel. Rather, they exhibit small wiggles or undulations. Dynamically, at short times, we have "nematic-elastic" (NE) modes. These are reminiscent of the Rouse modes in flexible isotropic chains because they occur on short timescales and are the fundamental modes of motion which the chain would have in the absence of entanglements or hydrodynamic interactions. The NE modes do not play an essential role in our analysis. However, at short enough time scales they are important. The NE modes involve small amplitude undulations of the chain about its equilibrium position. The simplest case to discuss is undulations about a perfectly straight chain. In general the calculation of the modes is not trivial because of the constraint of chain inextensibility. This constraint has an effect on the mobility matrix for a chain and implies that a force applied to one point on the chain has a complicated effect on other points on the chain, making the equations of motion non-linear. One way to calculate the mobility matrix (or its inverse - the friction matrix F) is to use the Rayleighian approach [32, 33, 4]. This is a generalisation of Lagrangian mechanics to the case of linear friction, and instead of calculating the Lagrangian one calculates the Rayleighian \mathcal{R} which is proportional to the kinetic energy of the chain. The equation of motion is then $\frac{\delta \mathcal{R}}{\delta \theta(s)} = -\frac{\delta U}{\delta \theta(s)}$ where U the chain energy (3). This yields

$$\int_{s'=0}^{s'=L} ds' F(s, s') \dot{\theta}(s') = \epsilon \frac{d^2 \theta(s)}{dt^2} - 3aS \sin \theta(s) \cos \theta(s). \quad (9)$$

If one linearises this about $\theta(s) = 0$ then the non-local nature of the equations disappears and one obtains, for an arbitrary perpendicular displacement Δ_{\perp} (with $\theta(s) = \frac{\partial \Delta_{\perp}(s)}{\partial s}$)

$$-\mu \frac{\partial \Delta_{\perp}(s)}{\partial t} = \epsilon \frac{\partial^4 \Delta_{\perp}(s)}{\partial s^4} - 3aS \frac{\partial^2 \Delta_{\perp}(s)}{\partial s^2}, \quad (10)$$

where s is the arc length measured from one end of the chain. The boundary conditions appropriate for this problem are:

$$\frac{\partial^2 \Delta_{\perp}(s)}{\partial s^2} = 0 \quad \text{and} \quad \epsilon \frac{\partial^3 \Delta_{\perp}(s)}{\partial s^3} = 3aS \frac{\partial \Delta_{\perp}(s)}{\partial s}, \quad (11)$$

at both ends of the chain. All the modes decay exponentially in time like $\exp(-t/\tau_n)$, with τ_n the decay time for the n th mode. The explicit forms for the modes are not particularly instructive. However, it is simple to write down the dispersion equation for a harmonic disturbance of wavevector q , by using $\Delta_{\perp}^q(s) \sim \exp(-t/\tau_q) \cos(qs)$ and (10) to give

$$\mu\tau_q^{-1} = \epsilon q^4 + 3aS q^2. \quad (12)$$

In the limit of long chains $L/\lambda \gg 1$ the longest lived mode involves a wavelength of about the length of the chain so $q \approx L^{-1}$. This gives a maximum characteristic time for NE dynamics of

$$\tau_{\text{NE}} = \frac{\mu L^2}{aS}. \quad (13)$$

One can calculate the amplitude \mathcal{A} of this longest-lived mode, by using $\Delta(s) = \mathcal{A} \cos(\pi s/L)$ in the energy equation (3) and equipartition ($k_B T/2$ per degree of freedom), which gives $\mathcal{A} \approx \sqrt{k_B T L / aS}$. Although the amplitude grows as $L^{1/2}$ the angle made by the chain with the director is $\sim \mathcal{A}/L$ which decreases with increasing chain length. The nematic elastic modes for a hairpinned chain will be similar to those for a straight chain. Some of these have been illustrated previously [4].

One can use the long wavelength mode to calculate how long the arms of a hairpin must be before their ends are likely to touch by vibrations of this kind. The answer, obtained by setting $\mathcal{A} \sim \lambda$ is $L/\lambda > U/(k_B T)$. In this, as in most of the previous studies of hairpins, a continuum model for the chain is used where the discreteness of the monomers is not accounted for. This means that one requires the hairpin length to be at least several monomers. If this is not the case there are some interesting effects associated with the discrete monomers. If we assume λ is many monomers in length then in a melt this implies each hairpin has many chains between its arms. Accordingly there will be physical barriers (the other chains) and probably entanglements, which present a dynamical barrier to the two ends meeting. We return to this below. However, the fact that such modes are excited means that a hairpin looks more like that in figure 1b rather than 1a. The perpendicular size of the polymer is [34, 35] roughly $\langle r_{\perp}^2 \rangle \sim L\lambda \left(\frac{U_h}{k_B T}\right)^{-1}$, when $U_h \gg k_B T$, so that in the perpendicular direction the polymer performs a random walk with step size $A = \lambda(k_B T/U_h)$. This can be obtained by considering only the longest wavelength mode described following equation (13). Another important fact is that the perpendicular extent of the polymer is due mainly to small meanderings of the chain. The hairpins, by themselves, each of size $\sim 2\lambda$, contribute $\sim n\lambda^2 \sim L\lambda U_h/k_B T \exp(-U_h/k_B T)$ to the lateral size of the chain. The ratio of the two contributions is $(U_h/k_B T)^2 \exp(-U_h/k_B T) \ll 1$, so that the encounter probability of the ends is essentially due to the small undulations.

The modes calculated above are the *internal* modes for the chain. The centre of mass is free to diffuse with diffusion constant $\sim k_B T/(\mu L)$. Of course, if there are entanglements a given chain sees a "tube" formed by these entanglements. Once a monomer has diffused a distance of the order of the tube diameter the NE modes are constrained. A similar situation occurs in the theory of melts of isotropic Gaussian chains [36] where there are four regimes of chain motion. At very short times the chain does not feel the tube constraints and undergoes free Rouse dynamics. At longer times it experiences the tube constraints and the motion perpendicular to the tube is suppressed. At yet longer times the motion is reptative, until the chain leaves

its tube and forms a new tube. For nematic PLCs we thus need to introduce another time τ_e which, for long enough chains must be smaller than τ_{NE} . For times $t < \tau_e$ the motion is governed by the NE modes. For $\tau_e < t < \tau_{NE}$ the NE modes are constrained. For $t > \tau_{NE}$ the reptative dynamics discussed in the next section dominates, at least until the chain leaves its original tube.

Because hairpins are geometrically so different from rod-like, slightly wiggly, or Gaussian chains one expects them to have rather large effects in some experiments. There have been many theoretical studies involving hairpins and several suggestions in the past for various experiments to detect them. These have included giant dielectric response [3], dielectric relaxation [4], effects on the elastic constants [5] and NMR [6]. One might also expect some effects on the rheology, but at present there is no rheological theory which includes hairpins. Despite all these suggestions there is as yet no conclusive experimental evidence that hairpins exist. The only evidence obtained so far involves some tantalising SANS measurements, which show a large increase in anisotropy at low temperatures [37] (see their Fig. 6). This is possibly due to the disappearance of hairpins as the temperature is decreased. One other possible piece of evidence occurs not in PLCs, but in ordinary polymers which are aligned by a shear flow [38]. It involves a long-time tail in the NMR linewidth decay following cessation of shear. This decay is much longer than the timescale expected from rheological measurements, and may be due to the presence of shear-induced hairpins.

3. Hairpin dynamics at long times.

In order to discuss the effect hairpins are likely to have on fluorescence and cyclisation experiments we first need to say something about hairpin dynamics at long times. There have been three previous studies of dynamics in the non-entangled regime [4, 6, 22] and some work on the dynamics of nematic chains without hairpins in melts [39, 40]. In this section we discuss the reptative dynamics, which involves motion of the hairpin arms over distances comparable to the length of the chain. Because of the nematic potential the “tube” for a nematic polymer is well approximated by a straight line (in the absence of hairpins) or a hairpin shape. This implies that the displacement undergone by a monomer in space is different from the isotropic melt case where the tube itself is a random walk. The nematic field also sets up its own tube [4] and this forces hairpin motion to be reptative irrespective of the entanglements. For times much longer than τ_{NE} diffusion parallel to the nematic field will occur much faster than that perpendicular to the field because the reptation is biased to chain configurations aligned along the field.

There are at least three possible experimental systems of interest. One can have: (i) a melt of flexible PLCs; (ii) a solution of flexible PLCs in a nematic solvent; and (iii) a blend of flexible PLCs and rod-like PLCs. In all cases one expects to find hairpins in the flexible chains. However, cases (ii) and (iii) may be difficult to achieve because of poor miscibility.

Case (ii) is the easiest to visualise, but is perhaps the most difficult mathematically. If the solution is dilute then there are no entanglements and a single hairpinned chain can move freely. In such a case, if we ignore hydrodynamic effects, the centre of mass motion and the internal motion decouple. The centre of mass motion is just a random walk with a diffusion constant scaling as L^{-1} . On long timescales the internal motion is modelled by the “two stick” theory [4]. In this model the arms of the hairpin are both straight and parallel, one of length s_1 and the other of length $L - s_1$. The bend length is neglected. The arms undergo free diffusion, but with a diffusion coefficient that depends on the arm length. The diffusion equation satisfied

by the probability distribution function $\psi(s_1)$ is

$$\frac{\partial \psi}{\partial t} = \frac{k_B T}{\mu} \frac{\partial}{\partial s_1} \left[\left(\frac{1}{s_1} + \frac{1}{L - s_1} \right) \frac{\partial \psi(s_1)}{\partial s_1} \right], \quad (14)$$

where t is time and μ is a microscopic friction constant (per unit length). The diffusion coefficient here is small when each of the arms have the same length, and diverges as one of the arms gets shorter. This makes the solution of problems involving this kind of dynamics mathematically unwieldy [6]. Yet the characteristic time for hairpin decay is $\tau_{\text{rep}} \sim \frac{\mu}{k_B T} L^3$ as one would expect. The motion is reptative, but without entanglements. It is the nematic field that creates the “tube”. The strange form of the diffusion coefficient in (14) arises because (14) is concerned with transfer of length between the arms. There are other equations associated with the random walk carried out by the centre of mass, but these do not affect the cyclisation. The extension of this model to the multi-hairpin case has also been considered [22]. We note here that the dynamics of similar kind of object, so called “kinks” which can be made in an extensional flow field has been considered recently [41, 42].

The dynamics in the entangled regime, which is expected to be important in case (i), has not been previously discussed. The hairpin is fixed in space by the entanglements, and the chain can only slither out of its tube. The diffusion constant is $D \sim k_B T / (\mu L)$ and the distribution function satisfies

$$\frac{\partial \psi}{\partial t} = \frac{k_B T}{L \mu} \frac{\partial^2 \psi}{\partial s_1^2}. \quad (15)$$

The characteristic time has the same scaling behaviour as for the unentangled regime.

Typically the reptation time τ_{rep} is much larger than the longest NE time, τ_{NE} , so one is justified in treating the two dynamical modes separately. The ratio of these two is $\tau_{\text{rep}} / \tau_{\text{NE}} \sim (U_h L) / (k_B T \lambda)$, but this is the same as the $\langle \delta \theta^2 \rangle$ where $\delta \theta$ is the angular deviation caused by the longest lived NE mode. Thus, the requirement that the hairpins are well defined (i.e. the chain is roughly straight) ensures that the dynamics separates into two regimes.

4. Cyclisation and fluorescence. Experiments. The effect of hairpins.

In this section we return to our main problem, cyclisation of nematic chains. We begin by discussing a melt of rods, which by definition cannot cyclise. However, the ends of two different labelled rods can meet and form an excimer and hence produce a detectable signal. The intensity of this signal scales as $[A^*]^2$ and should thus be distinguishable from any cyclisation effects, which scale as $[A^*]$. We then go on to consider the effect of hairpins. These of course permit cyclisation. We study their effects in three stages. Firstly we consider chains with at most one hairpin and where the arms are modelled as being perfectly straight. We then include the effect of arm meandering perpendicular to the nematic field. Finally we analyse the behaviour of chains with many hairpins.

Intermolecular excimer formation occurs when ends from two different chains meet. Below a certain “critical concentration” of labelled chains this effect will be negligible. Our aim here is to calculate this concentration, and we do so by considering chains without hairpins. These are approximated as a melt of rods. The system is excited at $t = 0$. For a chain which is effectively a rod the only way it can form an $(AB)^*$ is by meeting the correct end of another chain. Let us suppose there are c labelled chains per unit volume and hence the initial concentration of type A^* is also c . We assume that when an A^* and a B come within R_c , the capture radius, of one another, an excimer is formed. Then, at times larger than τ_{NE} each A^* end is performing a one dimensional random walk. The number of B ends per unit length originally available

for capture is cR_c^2 and the diffusion constant is $\sim k_B T / (\mu L)$. The characteristic time for the collision of two tagged ends is

$$\tau_a \sim \frac{\mu L}{c^2 R_c^4 k_B T}. \quad (16)$$

By making the concentration very low one can always ensure $\tau_a \gg \tau_s$ so that excited A* ends will decay spontaneously before meeting a B end. Thus the integrated excimer output is very small. The “critical concentration”, defined by $\tau_a \approx \tau_s$, is

$$c_c \sim \left(\frac{\mu L}{\tau_s R_c^4 k_B T} \right)^{\frac{1}{2}} \quad (17)$$

For $c > c_c$ binary rod-rod collisions are important and the integrated intensity scales as c^2 . The details of the calculation can be found in the appendix.

We have discussed only the dynamical contribution to the integrated signal. Of course initially there are some chain ends which are located within a reaction radius R_c of each other and do not need to move to react. These ends produce an “instantaneous” contribution to the signal of order $c^2 R_c^3$. This contribution will be negligible.

We now proceed to study intramolecular excimer formation, cyclisation, when the concentration of labelled chains is lower than c_c . In particular, we will calculate the rate constant $k(t)$ in the presence of hairpins. Of course, at any given temperature there is always a probability distribution for hairpins. At low temperatures there will be very few. As one increases the temperature the number of hairpins increases, but if the temperature is too high the chain approaches an isotropic random walk and the idea of having well defined hairpins ceases to be useful. Eventually, at high enough temperatures the nematic to isotropic transition takes place and hairpins, which by definition require large values of the order parameter, vanish entirely. We first study a melt of chains supporting at most one hairpin. Initially the analysis is based on a simple “two-stick” model for single hairpin dynamics.

The average distance between the ends on a single hairpinned chain scales as L . If the arms of the hairpin are totally straight and R_c is larger than the perpendicular distance between the arms i.e., a few λ , then the timescale for collisions is $\tau_{\text{rep}} \sim \mu L^3 / (k_B T)$. The collision dynamics for a single hairpin are different from the dynamics of rods considered in the Appendix. We need only consider one coordinate $w = |\Delta_{\parallel}|$, the distance between the ends of the chain. The probability distribution function $\psi(w)$ for unreacted ends satisfies

$$\frac{\partial \psi}{\partial t} = D \frac{\partial^2 \psi}{\partial w^2} + \delta(w - w_0) \alpha c_0 \quad (18)$$

and

$$\frac{dc_0}{dt} = -\alpha c_0 - D \left(\frac{\partial \psi}{\partial w} \right)_L \quad (19)$$

with

$$\int_0^L dw \psi(w) = c_1. \quad (20)$$

Here c_0 and c_1 are the number densities of chains with zero and one hairpins respectively, and D is the diffusion constant for single hairpin motion $D \sim (k_B T) / (\mu L)$. The first term on the RHS of (18) allows for the diffusive motion of hairpins along the chain. The second term, $\delta(w - w_0) \alpha c_0$, results from chains with no hairpins forming a hairpin which then has $w = w_0 \approx L$. This thermally activated creation of hairpins occurs with a rate α . Since the rate of hairpin annihilation in thermal equilibrium is $\sim \tau_{\text{rep}}^{-1}$, detailed balance [4] suggests that α

scales as τ_{rep}^{-1} . The delta function thus represents a source term. Hairpins are continually being created by thermal excitation at the end of the chain. Equation (19) follows from conservation of the number of chains. In (19) the α_0 term arises from zero-hairpin chains forming a hairpin, and thus being lost to the zero-hairpin chain population. The second flux term $-D\left(\frac{\partial\psi}{\partial w}\right)_L$ is caused by hairpins which fall off the end of the single hairpin chain and form zero hairpin chains. The boundary conditions on $\psi(w)$ are (19) combined with $\psi(0) = 0$, so that when the two arms have the same length excimer creation takes place. At $t = 0$ we have

$$c_0 = c(\Gamma + 1)^{-1} \quad c_1 = \Gamma c_0, \quad (21)$$

and

$$\psi(w, t = 0) = c_1 L^{-1}, \quad (22)$$

with Γ defined by (6). The reaction rate $\frac{dn}{dt}$ is just the flux at $w = 0$, so $\frac{dn}{dt} = D\frac{\partial\psi}{\partial w}$. At short times, $t \ll \tau_{\text{rep}}$, the zero hairpin chains do not have time to gain hairpins and to move these hairpins into reactive (equal-armed) configurations. One can show, using the propagator for a random walk, that their contribution is exponentially small in τ_{rep}/t . Thus, in this limit the source term in (18) is unimportant (unless Γ is very small). It is possible to calculate the reaction rate in different ways. We can estimate the flux from the fact that those hairpins near $w = 0$ undergo a random walk of length $\sim \sqrt{Dt}$ in time t . Half of these collide and so a hole of size \sqrt{Dt} opens up in the distribution function. The gradient produced is $\frac{\partial\psi}{\partial w} \sim c_1 L^{-1}/\sqrt{Dt}$. Hence the rate for short times is

$$\frac{dn}{dt} = -D\frac{\partial\psi}{\partial w} \sim -\sqrt{Dt}^{-1/2} \frac{c\Gamma}{L(\Gamma + 1)} \sim -\sqrt{\frac{k_B T}{\mu}} \frac{\Gamma}{\Gamma + 1} L^{-3/2} c t^{-1/2} \quad t \ll \tau_{\text{rep}}. \quad (23)$$

At long times, $t \gg \tau_{\text{rep}}$, another process becomes important: creation of hairpins on chains which originally had no hairpin. These chains, which originally had no possibility of cyclising, can now cyclise by shuffling length between their arms. Since the equations governing the dynamics are linear only the longest lived eigenmode is present for $t \gg \tau_{\text{rep}}$. The decay must then be exponential with characteristic time τ_{rep} so that $n(t) \sim c \exp(-t/\tau_{\text{rep}})$. The rate is thus

$$\frac{dn}{dt} \sim -c \frac{1}{\tau_{\text{rep}}} \exp(-t/\tau_{\text{rep}}) \quad t \gg \tau_{\text{rep}}. \quad (24)$$

Two things are clear from this simple calculation. Firstly, as one expects, for a low concentration of tagged chains both the reaction rate and the integrated signal scale linearly in c . This is because each chain is interacted with itself, rather than with other chains. Secondly, one might naively expect that increasing the chain length and hence the number of hairpins per chain would increase the integrated signal. This calculation suggests the opposite is true. Increasing the chain length does increase the number of hairpins because $\langle n \rangle \propto L$. However increasing L also slows the chain motion because the reptation time scales as L^3 .

So far, our discussion suggests the following picture. At low enough concentrations $c < c_c$ one expects the following behaviour as a function of L and c . For very small $L < \lambda$ a weak signal scaling as c^2 , followed by a region $L \gg \lambda$ where the signal scales as c , but decreases as with increasing L . This picture is however incomplete. As we shall see the large L behaviour is modified when one allows the presence of many hairpins. In particular, the L dependence of the integrated signal is $L^{-5/2}$. Also, our discussion, and most previous studies of nematic chains, applies only to long chains $L \gg \lambda$. It is necessary to analyse chain conformations in the region $L \leq \lambda$ and we do this in the next section. In the remainder of the present

section we elaborate the above analysis in three respects: (i) analyse the effect of perpendicular meanderings on the likelihood of reactive encounters between the tagged ends. (ii) In our earlier discussion the chains were confined to virtual tubes due to the nematic field. This field induces a strong alignment of the chains thus resulting in reptative dynamics even in the absence of entanglements. Yet, the presence of entanglements may further affect the dynamics by placing stronger barriers to lateral motion. As we shall see this leads to a different t dependence of $k(t)$ in the limit of small t . (iii) Finally we consider the cyclisation kinetics of chains with many hairpins ($n \gg 1$).

In the model presented above it was assumed that the arms were straight and parallel. As a result we also had to assume that the capture radius was a few hairpin lengths so that there was any chance of two ends meeting. If the arms were parallel and the capture radius satisfied $R_c < \lambda$ hairpins would definitely reduce the reaction rate because they would bunch the ends together, but not close enough to cyclise. Fortunately, as discussed in section 2, we know from the detailed calculations of Warner *et al.* [21] that the arms are not strictly parallel. The chain configuration in the perpendicular direction is a two-dimensional random walk of L/A steps each of length A with $A = \lambda k_B T / U_h$. Because $A \ll L$ the arms are sufficiently straight at low temperatures for the "rod-like" dynamics we have used to be valid. A hairpinned chain thus should be thought of as looking something like that in figure 1b rather than in figure 1a. The fact that the lateral extent scales as \sqrt{L} and is much greater than λ tells us that increasing L reduces the reaction rate. In an entangled system the random walk is essentially frozen-in and the only way two ends can meet is when a random walk with the two ends very close is generated. The fraction of walks which arrive after L/A steps within R_c of the origin may be obtained using the propagator for a two dimensional random walk of L/A steps, $G(\Delta r, L/A)$

$$\int_0^{R_c} dr r G(\Delta r, L/A) = \int_0^{R_c} dr r \left(\frac{2\pi LA}{3} \right)^{-1} \exp(-3r^2/2LA) \sim \frac{R_c^2}{LA} \ll 1. \quad (25)$$

Thus the instantaneous signal is decreased by a factor R_c^2/LA .

Although the static conformations of a chain's trajectory in the perpendicular direction are governed by the step size A it is not this step size which is important for the dynamics. Dynamically, once one is in the reptative regime it is the "primitive path" which is important, rather than the actual path taken by the chain. This is true both for nematic and for isotropic melts. The primitive path [36] is the shortest path which has the same topology as the actual chain with respect to entanglements. If N_E is the number of monomers between entanglements and N the degree of polymerisation of the chain, then the primitive path consists of $N_p = N/N_E$ "monomers" each of length $P = \sqrt{N_E} A$. We now need to include the effect of perpendicular meanderings of the primitive path on the reaction rate. To do this we refer to figure 3, which attempts to represent the distribution of end to end distances along the three axes. Initially, at $t = 0$ there is a spherical hole of radius R_c which occurs because of the ends located within a reaction radius (Fig. 3a). We now run the experiment for a short time t . For ends to react in this time they must have $\Delta z < (Dt)^{1/2}$, and $\Delta x < P^{1/2}(Dt)^{1/4}$, $\Delta y < P^{1/2}(Dt)^{1/4}$, where the z axis is parallel to the director. This defines an ellipsoid which is shown in figure 3c. At times greater than the time to diffuse an entanglement length the major axis of the ellipsoid is located along the z axis. At very short time $< R_c^4 P^{-2} D^{-1}$ the ellipsoid looks like 3b, but at such short times our dynamics becomes unphysical, so we need only concern ourselves with figure 3c. The volume between the ellipsoid and the sphere is just $V \sim PDt - R_c^3 \approx PDt$. The fraction of chain ends within this sphere is $\sim L^{-1}(LP^{-1}P^2)^{-1}V \sim k_B T t / (\mu L^3) \sim t / \tau_{rep}$. Thus the reaction follows $\frac{dn}{dt} = -(\tau_{rep}^{-1})n$, and the rate constant at short times is a constant $k(t) \sim \tau_{rep}^{-1}$.

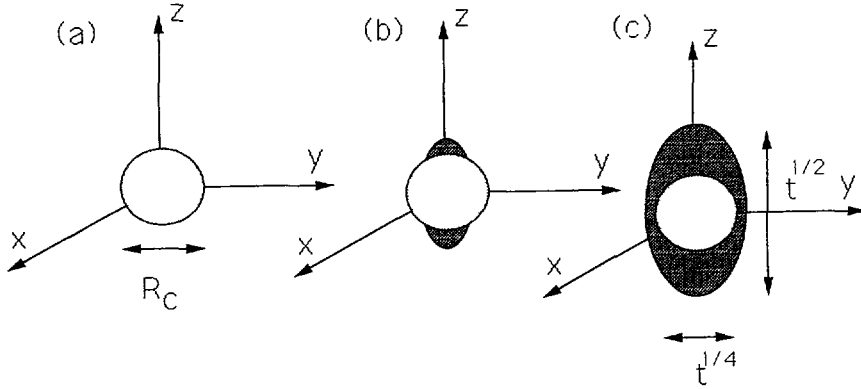


Fig.3. — Three pictures of the “hole” opened up in the end-to-end distribution function for single chains. The z axis is the director axis. Initially (a) there is a hole of radius equal to the capture radius where there are no ends. The ends then start to diffuse. At short (unphysical for our reptative model) times the situation is like that shown in (b). In (c) an ellipsoid has formed where there are few chain ends. The long axis of the ellipsoid is along the director because the chain motion is most rapid in that direction.

Expressed as a function of the total concentration of labelled chains, c , it is $k(t) \sim \tau_{\text{rep}}^{-1} \frac{\Gamma}{\Gamma + 1}$. Thus the reaction is initially described by an exponential decay. The rate is slower than that suggested by the “two-stick” approximation for which the reaction rate had a singularity at the origin. At long times the decay must also be exponential with time constant $\sim \tau_{\text{rep}}$.

This situation is somewhat similar to the case of reptative motion in *isotropic* melts studied by Bernard *et al.* [12, 13]. Using the Doi-Edwards earthworm equations [43] these authors found the exact reaction rate constant $k(t)$. At times short compared to the reptation time $t \ll \tau_{\text{rep}} \sim \mu L^3 / (k_B T)$ it scales as $\sim \tau_{\text{rep}}^{-1} (t/\tau_{\text{rep}})^{-1/4}$, whereas at long times it becomes constant $\sim \tau_{\text{rep}}^{-1}$. These scaling relations can be derived fairly easily. The long time behaviour, which must be exponential decay with time constant $\sim \tau_{\text{rep}}$ has already been discussed [13]. The short term behaviour is caused by one well known fact [36]. For a primitive chain reptating in a tube the arc-length distance travelled is proportional to $t^{1/2}$. However, the primitive path is itself a random walk, and thus in travelling an arc-length distance s the displacement in real space scales as $s^{1/2}$. Thus the displacement is $bt^{1/4}$, where b is a constant. We now imagine the experiment is run for a short time Δt . In this time only ends which are located within a sphere of radius $\Delta x = b\Delta t^{1/4}$ can meet. The number of such ends, (assuming $\Delta x \ll \sqrt{N_p}P$) is $\propto \Delta x^3$. Thus the number of end collisions in time Δt is $\propto \Delta t^{3/4}$, and hence the reaction equation at short times is $\frac{dn}{dt} = -k(t)n$ with $k(t) \sim \tau_{\text{rep}}^{-1} (t/\tau_{\text{rep}})^{-1/4}$, where we have inserted factors of τ_{rep} on dimensional grounds.

On a chain of length $L \gg \lambda$ there is always a possibility of finding $n > 1$ hairpins, given by (8). What is the effect of a large number of hairpins? Because the length is unchanged the diffusion constant is the same. As stated above the end to end distance along the normal to the director is also unchanged since it depends mainly on the perpendicular meandering behaviour. However, the distribution of end to end distances along the director does change. In the case of a single hairpin we argued it was uniform between $-L$ and L . It is known [21, 22] that the parallel end to end distance scales as $Ln^{-1/2}$ for large n . The distribution must thus be peaked about $\Delta_{\parallel} = 0$. This can be seen qualitatively by considering figure 4. One takes

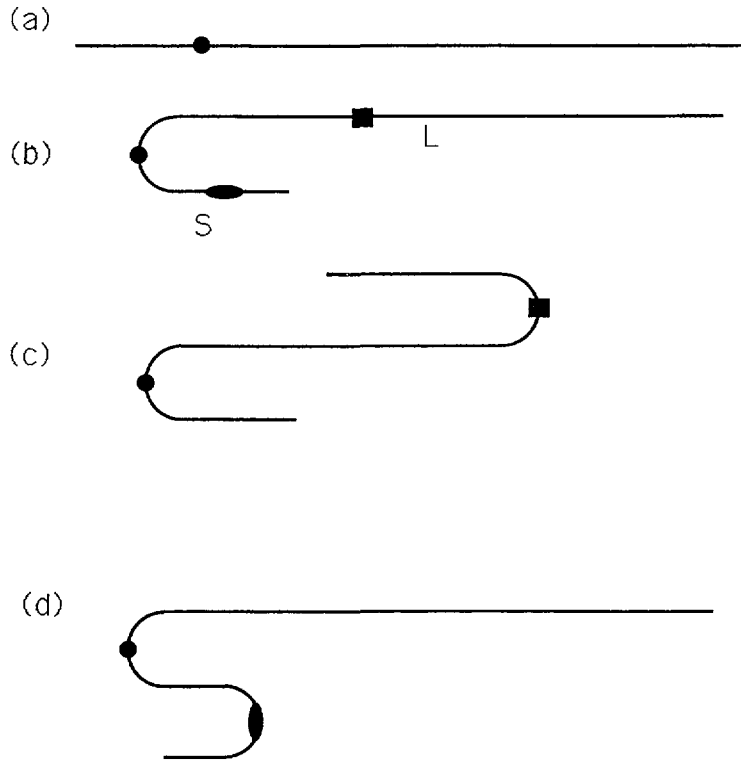


Fig.4. — A pictorial explanation for the peak in the parallel end to end distance distribution $|\Delta_{||}|$ in the presence of more than one hairpin. In (a) the first hairpin (represented by the black sphere) can be placed anywhere, giving a uniform distribution for $|\Delta_{||}|$ and forming a hairpin like that shown in (b). However, the next hairpin has a far greater probability of being placed on the long arm (L) (say where the black box is) and forming the shape shown in (c), rather than on the short arm (S) (where the oval is) and forming the shape in (d). It is clear by comparing (c) and (d) that this produces a bias towards small $|\Delta_{||}|$.

a perfectly straight chain and represents the hairpins by points on the chain. We place one point on the chain and bend the chain over at this point. Because this first point is placed randomly $\Delta_{||}$ has a uniform distribution. Now we take another point and place it randomly on the chain. It could either be placed on the long arm (L) or the short arm (S), forming the two possibilities shown in 4c and 4d. Since the long arm is longer the hairpin is much more likely to be placed there and hence make $\Delta_{||}$ smaller. Thus, for $n > 1$ hairpins, small end to end distances are favoured. The width of the distribution of $|\Delta_{||}|$ changes from L , for the one hairpin case, to $Ln^{-1/2}$ ($n \gg 1$). Also, the number of ends near $|\Delta_{||}| = 0$ is increased by a factor of \sqrt{n} . Altogether the concentration of uncyclised chains with n hairpins, c_n , is obtained from our single hairpin result, multiplied by \sqrt{n}

$$\frac{dc_n}{dt} \sim -n^{1/2} \tau_{\text{rep}}^{-1} c_n \quad n \gg 1. \quad (26)$$

Thus the rate of cyclisation for a chain of fixed length grows with the number of hairpins. Of course such hairpins are thermally activated. Thus cyclisation is not dominated by fluctuations

with $n > \langle n \rangle$. We can now discuss the case of very long chains. On a long chain the average number of hairpins is $\langle n \rangle = Ll^{-1} \exp(-U_h/k_B T)$. The distribution function is strongly peaked about this number so we can assume that there are only chains with $\langle n \rangle$ hairpins. At short times the rate constant for cyclisation is then (using (26))

$$k \sim \sqrt{aSL}^{-5/2} (k_B T)^{1/2} \exp(-U_h/2k_B T) \quad \langle n \rangle \gg 1 \quad (27)$$

and because this is a constant the decay is initially exponential with this as the inverse time. There are three things to note about (27). Firstly k is time independent. Secondly, k decreases steeply with chain length. Thus, while hairpins favour cyclisation of long chains by reducing the parallel end to end distance, this effect is overwhelmed by the dynamics. Finally, the reaction rate has a very strong dependence on temperature. This exponential type dependence is typical of many chain properties which depend on hairpins, in particular the giant dielectric response prediction [3]. From (26) we can derive the integrated intensity \mathcal{I} . This is

$$\mathcal{I} = \int_0^\infty dt \exp(-t/\tau_s) \sum_{n=0}^\infty \frac{dc_n}{dt} \quad (28)$$

where we have summed over all possible hairpin numbers n . We know the time evolution is $c_n(t) = c_n(0) \exp(-t/\sqrt{n}\tau_{\text{rep}})$ where the distribution function $c_n(0) = cP(n)$ and $P(n)$ is given by (8). $P(n)$ for large Γ is effectively a delta function peaked about $n = \langle n \rangle = \Gamma$ and so (assuming $\tau_s \ll \Gamma\tau_{\text{rep}}$) the integrated signal is

$$\mathcal{I} \sim c\tau_s \Gamma^{1/2} \tau_{\text{rep}}^{-1} \propto cL^{-5/2} \quad (29)$$

We have $\mathcal{I} \sim k$ and the integrated signal measures the rate constant.

5. Ringlets.

Our discussion so far has suggested no cyclisation mechanism for short chains. For long chains $L \gg \lambda$ we know that the cyclisation rate is a decreasing function of L . However, we have been able to say little about chains with $L \approx \lambda$, in part because previous hairpin studies have been usually restricted to $L \gg \lambda$. Here we will show the cyclisation rate is expected to be maximal for $L \approx \lambda$. The regime $L \approx \lambda$ is in fact of some intrinsic interest in itself, independent of any reaction rate effects. For linear chains it is known that the lowest energy state corresponds to a chain aligned along the nematic director, and that the excited equilibrium states are hairpins [20, 4]. One can ask exactly the same questions for cycles. What is the ground state of such a chain and what are its excited states? In this section we answer the first part of this question and predict a new object, a "ringlet" for which the cyclisation rate is maximal. We begin with energy functional of a chain with trajectory $\theta(s)$ (3). To find the equilibrium states for a closed loop we need to extremise this functional subject to two constraints. Firstly, that we begin and end at the same point in space

$$\int_0^L ds \cos \theta(s) = \int_0^L ds \sin \theta(s) = 0. \quad (30)$$

We also need to impose continuity of the tangent vector

$$\theta(L) = \theta(0) + 2n\pi \quad n \text{ an integer}, \quad (31)$$

to avoid an infinite bending energy at the point of discontinuity. Now it is feasible to extremise (3) subject to constraints (30) by introducing two Lagrange multipliers, μ and ω for

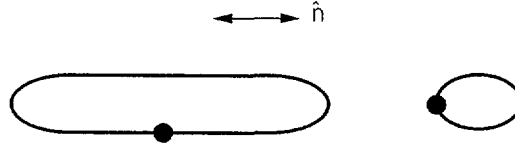


Fig.5. — The possible ground states for a cyclised chain. A long chain (left) will want to form the double hairpin configuration. A short chain (right) will form a ringlet. One should note that both these objects are actually the lowest energy states for a cyclised chain. This should be contrasted with a non-cyclised chain which has as its ground state a straight line aligned along the director.

the constraints. This would reduce the problem [23] to one of a classical particle moving in a potential

$$u(\theta) = -3aS \sin^2 \theta + \mu \cos \theta + \omega \sin \theta. \quad (32)$$

The solutions for the extremal trajectories will be complicated elliptic functions [23]. However a semi-quantitative analysis yields the information we seek. By definition the lowest energy state of this cyclised system is not a straight line. In the limit $L \gg \lambda$ the lowest energy state will be the double-hairpin configuration of energy $2U_h$, shown in figure 5, because for such a state the chain is mainly aligned along the director. In the limit of $L \approx \lambda$ the exact shape taken by the ground state is unknown, but we can approximate it crudely by a circle $\theta(s) = 2\pi s/L$. The energy of such a circle is

$$U_r(L) = U_h \left[\pi^2 \left(\frac{\lambda}{L} \right) + \frac{1}{8} \left(\frac{L}{\lambda} \right) \right] \quad (33)$$

We now ask the following question: is there a chain length L which yields the ground state with the lowest energy? For the assumed circular shape there is a minimum at

$$L_{\min} = 2\sqrt{2}\pi\lambda, \quad (34)$$

with an energy of

$$U_{\min} = \frac{\pi}{\sqrt{2}}U_h < 2U_h. \quad (35)$$

Thus a cyclised chain of length $\frac{\pi}{\sqrt{2}}\lambda$ certainly has a lower energy ground state than an infinitely long chain for which the ground state is two hairpins. There are now two possibilities. Either the minimum energy occurs for $L \sim \lambda$ and its energy is $\sim U_h$ or the minimum energy occurs as $L \rightarrow 0$ and is $U \rightarrow 0$. This reasoning is based on the fact that there is only one length scale, λ , and one energy, U_h , in the problem. It is easy to exclude the zero length possibility by examining the bending term. From an elementary inequality of calculus (the CBS inequality [44]) we know the bending energy satisfies

$$\frac{\epsilon}{2} \int_0^L ds \left(\frac{d\theta}{ds} \right)^2 \geq \frac{\epsilon}{2} \frac{1}{L} (2n\pi)^2 \quad (36)$$

where n is the number of loops. For a simple closed curve this is just 1. Since (36) diverges as $L \rightarrow 0$ any small loop always has a very large energy, due to the bending term. For short lengths the bending energy is very large, whilst for long lengths the nematic energy can become large. Thus the chain length which gives the minimum energy is $L \sim \lambda$ and this minimum energy is σU_h where $0 < \sigma \leq \frac{\pi}{\sqrt{2}}$. Like a hairpin this minimum is a balance between the

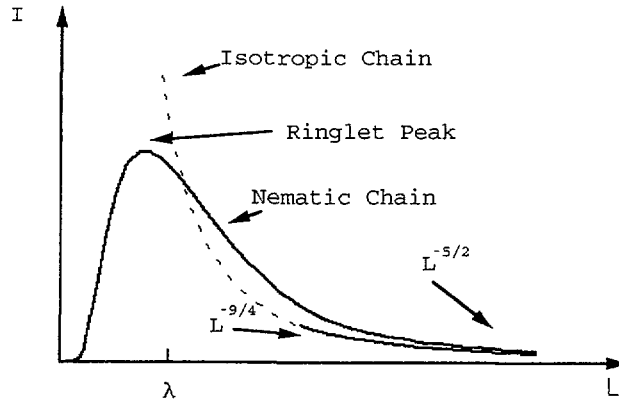


Fig.6. — A sketch of the integrated signal versus chain length for a nematic chain and an isotropic chain. For the nematic chain at very small chain lengths $L \ll \lambda$ the bending penalty is too great for intramolecular cyclisation. At long lengths where there are many hairpins the integrated signal should decrease as $L^{-5/2}$. At lengths close to a few λ there will be a strong ringlet peak. For the isotropic chain undergoing reptative motion we expect $I \sim L^{-9/4}$. The dotted line represents deviations from reptative motion caused by the Rouse modes. The exact position of intersection with the nematic curve is not known.

nematic and bending terms. In keeping with the usual hairdressing terminology [20, 23] of this field we shall refer to this minimum energy loop as a “ringlet” (see Fig. 5).

These ringlets are significant in the cyclisation problem because we know that for rods cyclisation rate $\frac{dn}{dt}$ is zero. A maximum is thus expected at some intermediate L . We also know that $\frac{dn}{dt}$ for long chains decreases with increasing chain length, despite the presence of hairpins. In this section we identify the maximum in the cyclisation rate at $L \sim \lambda$ with ringlet formation, providing $k_B T < U_h$ and $R_c \ll \lambda$. Chains of length $\ll \lambda$ cannot cyclise because the bending penalty is too large and the rate is controlled by a Boltzmann factor. Chains of length $L \gg \lambda$ can cyclise, but the rate of cyclisation is slow because of the reptational dynamics. Cyclisation in the vicinity of the maximum $L \approx \lambda$ gives rise to an integrated signal of the form $f(L, k_B T) \exp(-U(L)/(k_B T))$ where f is a weak function of L and $U(L)$ has roughly the form of $U_r(L)$ (33) (see Fig. 6). The exact form of f depends on the dynamics. For small L , below the entanglement threshold, the NE modes will dominate the dynamics. At large L , and at long times reptative dynamics control f . What is clear is that the dependence on L is weak compared to the exponential dependence of the second term. The maximum in the integrated signal is then very close to $L \sim \lambda$ when $k_B T < U_h$. The above statements are subject to the following caveat. The hairpin length was assumed to be much greater than a monomer length. If this condition is not satisfied the discrete nature of the chain can have quantitative effects [4].

A similar effect has been seen previously, experimentally and theoretically, in wormlike chains with no nematic field and in DNA fragments [45-48]. For isotropic chains with finite persistence length the peak in the cyclisation rate balances two effects. At short lengths the chain rigidity decreases the cyclisation probability. At long lengths there is a phase space effect. A chain with N monomers has a smaller chance of returning to its starting point as N grows. There is thus a peak in the cyclisation rate for chains roughly one persistence length long. The analysis reported relied on chain statics rather than dynamics.

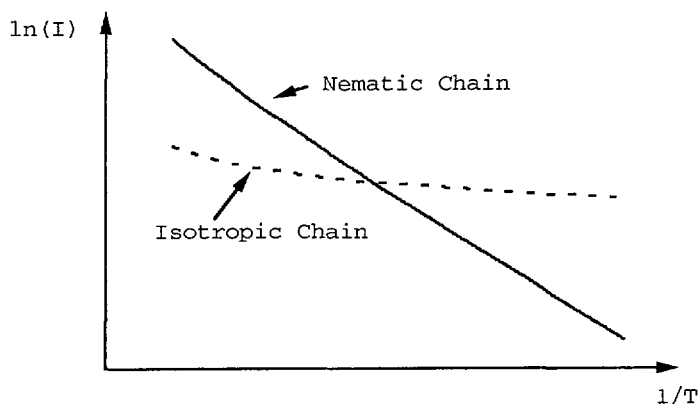


Fig.7. — A sketch of the logarithm of the integrated signal versus reciprocal temperature for a nematic and an isotropic chain. Both undergo reptative motion. For the nematic chain the temperature dependence is $\mathcal{I} \sim T^{1/2} \exp(-U_h/2k_B T)$ which dominates the isotropic result at small $1/T$ because of the creation of hairpins. The expected result for an isotropic chain is $\mathcal{I} \sim T^{3/4}$

6. Discussion and conclusion.

Nematic polymers can hardly cyclise when their length is short compared to their persistence length. Formation of hairpins enables cyclisation by allowing the ends to approach each other. If we vary the chain length then an interesting effect occurs. At very short chain lengths the bending term in the chain energy prevents cyclisation. At large chain length lengths, although hairpin formation is favoured the cyclisation decreases rapidly with chain length. This is for dynamical reasons - the reptation time increases as L^3 and slows the cyclisation rate by this factor. It is clear then that the cyclisation rate must reach a maximum at some chain length (Fig. 6). What we propose is that this occurs for a chain of a few hairpin lengths. Such chains can form "ringlets" which are the minimum energy shape for a closed chain. Because of the Boltzmann factor responsible for ringlet formation we argue that this conclusion is not sensitive to the details of the dynamics. Thus the cyclisation peak should always be around the ringlet length irrespective of whether reptation or Rouse-like behaviour governs their dynamics. The ringlet peak is absent in ordinary isotropic Gaussian polymer systems where the rate constant always decreases with increasing chain length. For chains of constant length the reaction rate is predicted to depend exponentially on the temperature (Fig. 7). This is because the production of hairpins requires an activation energy. In turn, the end to end distance decreases as the number of hairpins grows, thus favouring cyclisation. This exponential dependence on temperature is typical of many chain properties which are hairpin dependent, such as the radius of gyration along the nematic director or the dielectric response. Any physical property which depends on the number of hairpins, even weakly, will always show a very strong temperature dependence.

The N and T dependence of the cyclisation rate are qualitatively different from the cyclisation dynamics of isotropic chains where the reaction decreases monotonically with chain length, and the temperature dependence is weak. These results suggest the use of excimer fluorescence as a probe for hairpin formation. Such an endeavour is of interest because of the paucity of experimental evidence for the existence of hairpins. At the same time such experiments can test the validity of current ideas concerning the dynamics of nematic polymers. Ideally, the

experiments should test both the T and the N dependence. However, in melt conditions one should allow for the effect of N and T on the nematic order parameter which itself affects the characteristic lengths and energies in the problem. One should also avoid a change of phase as T and N are varied. By definition, hairpins exist only in the well-ordered nematic phase with order parameter $S \approx 1$.

There are essentially two parts to the cyclisation problem. The first involves equilibrium statistical mechanics of the chain ends. Only for a hairpin and a ringlet are the chain ends close together. For a rod this is impossible, and for a chain which has no hairpins it is very unlikely. The second contribution, which determines the precise time behaviour, arises from the dynamics. Given that two ends are a certain distance apart at $t = 0$ we need to find when they will collide. This depends on the timescales we are interested in. In this paper we have assumed that measurements can be made on timescales for which reptative motion becomes important. This implies that long-lived fluorescent tags are needed. However, qualitatively we expect similar results for motion based on the NE modes or any other short-time behaviour. Clearly, a direct test of the theoretical predictions presented above requires samples of low polydispersity. We note however that the detection of excimer formation in a dilute nematic sample of tagged chains is a qualitative test for the occurrence of hairpins.

One other possible experimental effect might involve the use of nematic chains which also have electric dipoles in the backbone [3, 23]. By applying a strong electric field to such a polymer one expects an exponential decrease in both hairpin and ringlet formation and hence an large decrease in the cyclisation rate.

Acknowledgements.

DRMW and AH enjoyed financial support provided by DOE grant DE-FG03-87ER45288 and the Ford Motor Co. DRMW thanks Mark Warner for introducing him to, and for many useful discussions on the subject of nematic polymers. AH benefitted from useful discussions with M. Winnik. This work was carried out under the auspices of the KFJ foundation.

Appendix.

Excimer fluorescence from rods.

Here we calculate the reaction rate for excimer formation when we have a dilute solution of labelled rods. Naturally, such excimer formation cannot occur by cyclisation, but only by two different rods meeting. As explained in section 4 the rods undergo one-dimensional diffusion. One can say something quantitative by using the theory for diffusion limited reactions developed by de Gennes [14, 15]. Because we have ordinary diffusion in one dimension the process is "compact" - each possible site is visited many times by the chain end. Let the number density of A ends which have not yet contacted a B end be n_A . The number of such

ends per unit length is then $n_A R_c^2$ and we have

$$\frac{dn_A}{dt} = -k(t)n_A^2, \quad (37)$$

where $k(t)$ is a time dependent rate constant. We are in one dimension $d = 1$ and have ordinary diffusion, so that in time t each rod moves a distance $\sim t^u$ with $u = 1/2$. From the general formula $k \sim t^{u d - 1}$ [14] we have

$$k(t) = R_c^2 t^{-1/2} / (\sigma \pi), \quad (38)$$

where σ is a constant. The number density of ends thus satisfies

$$n_A(t) = (c^{-1} + 2t^{1/2} R_c^2 / \sigma \pi)^{-1} \quad (39)$$

On dimensional grounds the constant σ is approximately $\sqrt{\mu L / k_B T}$. The reaction rate $\frac{dn}{dt}$ is

$$\frac{dn}{dt} \propto -\frac{dn_A}{dt} = \frac{(R_c^2 / (\sigma \pi)) t^{-1/2}}{(c^{-1} + 2\sqrt{t} R_c^2 / (\sigma \pi))^2}. \quad (40)$$

At times short compared to the characteristic time τ_a (16), $t < \tau_a$

$$\frac{dn}{dt} \sim c^2 R_c^2 \sigma^{-1} t^{-1/2} \sim \left(\frac{c}{\tau_a}\right) \left(\frac{t}{\tau_a}\right)^{-1/2}, \quad (41)$$

and at long times $t > \tau_a$

$$\frac{dn}{dt} \sim t^{-3/2} \sigma R_c^{-2} \sim \left(\frac{c}{\tau_a}\right) \left(\frac{t}{\tau_a}\right)^{-3/2} \quad (42)$$

Thus at long times $\frac{dn}{dt}$ is independent of c . The reaction is initially very fast, but the reaction rate declines rapidly because the supply of initially close ends is quickly exhausted. The time τ_a marks roughly the half-way point of the reaction, so that roughly half the ends have collided by then. At very short times the analysis used here breaks down because then the NE modes become important. Also, at very long times the diffusion is not entirely in one dimension and the ends can explore the full three dimensional volume, albeit with a very anisotropic diffusion constant. If $\tau_a \ll \tau_s$ essentially all the ends meet in the time it takes the A* ends to decay spontaneously. If however $\tau_a \gg \tau_s$ very few end meet before spontaneous decay, and the integrated signal is small. It is now easy to calculate the integrated intensity \mathcal{I} . If the spontaneous decay is slow then

$$\mathcal{I} \sim c[1 - \mathcal{O}(\tau_a/\tau_s)^{1/2}] \quad \tau_a \ll \tau_s. \quad (43)$$

In this case of course almost all the rods meet so the leading term scales as the number of rods. In the case where the spontaneous decay is fast one obtains

$$\mathcal{I} \sim c \left[\sqrt{\frac{\pi}{\lambda_s \tau_a}} - \frac{1}{\lambda_s \tau_a} \exp(-\lambda_s \tau_a) \right] \quad \tau_a \gg \tau_s. \quad (44)$$

In this regime the integrated signal scales as $c^2 \sqrt{\frac{k_B T}{\mu L}}$. Thus, since $\tau_a \propto c^{-2}$, by reducing the concentration one can easily get into a regime where $\tau_a \ll \tau_s$ and the integrated signal is small.

Note however a complication which is missing from this theory. Each chain has of course two ends. If one end is cyclised and remains joined for a long time (i.e. if τ_E is large) then it affects the dynamics of the other ends by making the chain twice as long. We have ignored this rare process and its generalisations to larger numbers of chains.

References

- [1] A. Ciferri, W.R. Krigbaum, R.B. Meyer Eds., *Polymer Liquid Crystals*, (Academic, New York, 1982).
- [2] A. Ciferri Ed., *Liquid Crystallinity in Polymers*, (VCH, New York, 1991).
- [3] Gunn J.M.F., Warner M., *Phys. Rev. Lett.* **58** (1987) 393.
- [4] Williams D.R.M., Warner M., *J. Phys. France* **51** (1990) 317.
- [5] Selinger J.V., Bruinsma R.F., Preprint *Statistical Mechanics of Defects in Polymer Liquid Crystals*.
- [6] Warner M., Williams D.R.M., *J. Phys. II France* **2** (1992) 471.
- [7] Wilemski G., Fixman M., *J. Chem. Phys.* **60** (1974) 866.
- [8] Wilemski G., Fixman M., *J. Chem. Phys.* **60** (1974) 878.
- [9] Doi M., *Chem. Phys.* **11** (1975) 107.
- [10] Doi M., *Chem. Phys.* **11** (1975) 115.
- [11] Doi M., *Chem. Phys.* **9** (1975) 455.
- [12] Bernard D.A., Noolandi J., *Phys. Rev. Lett.* **50** (1983) 253.
- [13] Noolandi J., Hong K.M., Bernard D.A., *Macromolecules* **17** (1984) 2895.
- [14] de Gennes P.G., *J. Chem. Phys.* **76** (1982) 3316.
- [15] de Gennes P.G., *J. Chem. Phys.* **76** (1982) 3322.
- [16] Winnik M.A., *Molecular Dynamics in Restricted Geometries*, J. Klafter, J.M. Drake Eds. (John Wiley, New York, 1987).
- [17] Winnik M.A., *Acc. Chem. Res.* **18** (1985) 73.
- [18] Winnik M.A., *Chem. Rev.* **81** (1981) 491.
- [19] Horie K., Mita I., *Macromolecules* **11** (1978) 1175.
- [20] de Gennes P.G. in [1].
- [21] Warner M., Gunn J.M.F., Baumgärtner A.B., *J. Phys. A.* **18** (1985) 3007.
- [22] Williams D.R.M., Warner M., *Computer Simulation of Polymers*, R.J. Roe Ed. (Prentice Hall, Englewood Cliffs, 1991).
- [23] Williams D.R.M., *J. Phys. A.* **24** (1991) 4427.
- [24] Lo W.S., Pelcovits R.A., Preprint: *Nonlocal Elasticity Theory of Polymeric Liquid Crystals*.
- [25] Le Doussal P., Nelson D.R., Preprint: *Statistical Mechanics of Directed Polymer Melts*.
- [26] Selinger J.V., Bruinsma R.F., *Phys. Rev. A* **43** (1991) 2910.
- [27] Croxton C.A., *Macromolecules* **24** (1991) 537.
- [28] Toner J., Preprint *Breakdown of elasticity theory in nematic polymers*.
- [29] Petschek R.G., Terentjev E.M., *Phys. Rev. A.* **45** (1992) 930.
- [30] Croxton C.A., *Polym. Commun.* **31** (1990) 45.
- [31] Croxton C.A., *Polym. Commun.* **32** (1991) 66.
- [32] Lord Rayleigh, *The Theory of Sound*, (Dover, New York, 1945).
- [33] Pars L.A., *A Treatise on Analytical Dynamics*, (Wiley, New York, 1965).
- [34] Warner M., Gelling K.P., Vilgis T.A., *J. Chem. Phys.* **88** (1988) 4008.
- [35] Note: The original result for $\langle r_{\perp}^2 \rangle$ in [21] (their Eq. (5.14)) is incorrect. The result is corrected in [34] (Eq. (17b)).
- [36] Doi M., Edwards S.F., *The Theory of Polymer Dynamics*, (Clarendon, Oxford, 1986).
- [37] D'Allest J.F., Sixou P., Blumstein A., Blumstein R.B., Teixeira J., Noirez L., *Mol. Cryst. Liq. Cryst.* **155** (1988) 581. ;
D'Allest *et al.*, *Phys. Rev. Lett.* **61** (1988) 2562.
- [38] Nakatani A.I., Poliks M.D., Samulski E.T., *Macromolecules* **23** (1990) 2686.

- [39] Semenov A.N., *Sov. Phys. JETP* **66** (1987) 712.
- [40] Semenov A.N., Preprint on worm-like dynamics for nematics.
- [41] Larson R.G., *Rheol. Acta.* **29** (1990) 371.
- [42] Rallison J.M., Hinch E.J., *J. Non-Newtonian Fluid Mech.* **29** (1988) 37.
- [43] Doi M., Edwards S.F., *J. Chem. Soc., Faraday Trans. 2* **74** (1978) 1789.
- [44] Kazarinoff N.D., *Analytic Inequalities* (Holt, Rinehart and Winston, N.Y., 1961).
- [45] Gobush W., Yamakawa H., Stockmayer W.H., Magee W.S., *J. Chem Phys* **57** (1972) 2839.
- [46] Yamakawa H., Stockmayer W.H., *J. Chem Phys* **57** (1972) 2843.
- [47] Shore D., Baldwin R.L., *J. Mol. Biol.* **170** (1983) 957.
- [48] Shore D., Baldwin R.L., *J. Mol. Biol.* **170** (1983) 983.